In the structurally similar zeolite ferrierite, where 4 peaks of relative intensities 8:8:4:16 are to be expected, two peaks of relative intensities 4:5 (16:20) are observed due to overlap. For highly siliceous faujasite, a single line has previously been reported[7] corresponding to the single unique environment identified by X-ray diffraction.[13] It is probable that the chemical shifts are related to the "tetrahedral" bonding around the silicon atom in terms of deviations from perfect tetrahedral symmetry and/or Si-O-Si angles in these highly siliceous systems, and it may be possible in the future to make more quantitative comparisons between the results of the NMR and X-ray diffraction techniques. Substantial efforts are currently being made in this area[14] to refine the XRD data for the completely siliceous systems to provide detailed structures with accurate bond lengths and angles (XRD data on low Si/Al ratio zeolites will be inaccurate due to averaging over the Si/Al distribution of the various sites) and to compare these with the ^{29}Si chemical shift data found in this work. It is probable that such a correlation will be found and may be used to investigate zeolites of unknown structures if highly siliceous forms can be prepared. In addition, the well-resolved spectra of highly siliceous systems and their characteristic chemical shifts may make possible the study of mixed zeolites and intergrowths by NMR techniques.

Acknowledgment. The authors extend their appreciation to F. Sammut for experimental work. They also acknowledge the financial assistance of the Natural Sciences and Engineering Research Council of Canada in the form of Operating and Strategic Research Grants (C.A.F.) and a Graduate Scholarship (G.C.G.) and Imperial Oil Ltd. of Canada for a University Research Grant (C.A.F.). The high-field MAS NMR spectra were obtained with use of the facilities of the South Western Ontario High-Field NMR Centre, Manager, Dr. R. E. Lenkinski. Dr. R. I. Gait of the Royal Ontario Museum and Dr. W. Chesworth and Dr. J. A. Apps are thanked for their assistance in providing the mineral samples studied.

Registry No. ^{29}Si, 14304-87-1; albite, 12244-10-9; natrolite, 1318-95-2; microcline, 12251-43-3.

(13) Baur, W. H. *Am. Mineral.* **1964**, *49*, 697.
(14) Fyfe, C. A.; Murphy, W. J.; et al., work in progress.

Proton NMR Studies of the Electronic and Molecular Structure of Ferric Low-Spin Horseradish Peroxidase Complexes

Jeffrey S. de Ropp, Gerd N. La Mar,* Kevin M. Smith, and Kevin C. Langry

Contribution from the Department of Chemistry, University of California, Davis, California 95616. *Received February 13, 1984*

Abstract: High-field proton NMR studies of native and reconstituted horseradish peroxidase (HRP) were used to investigate the electronic and physical structure of the heme pocket in three ferric low-spin forms of the protein. Reconstitution of selectively deuterium labeled hemes into apo-HRP led to the definitive assignment of many hyperfine shifted peaks. Consideration of line width, pH titration data, and the effect of heme peripheral substituents has permitted the assignment of additional heme as well as proximal histidine peaks. Variable temperature data present further evidence of tight heme-apoprotein contacts in HRP. It is shown that the transition of the cyanide complex of HRP at high pH to a new cyanide-ligated alkaline form is consistent with a change in axial magnetic anisotropy. At high pH resting state HRP undergoes a more drastic change in spectrum and structure that is attributed to coordination of a distal histidine in a configuration with its imidazole deprotonated and its π plane oriented essentially perpendicular to that of the proximal histidyl imidazole.

Horseradish peroxidase, HRP (E.C. 1.11.1.7), is a heme b protein obtainable from horseradish roots whose biological function, in common with other peroxidases, is the reduction of hydrogen peroxide produced in vivo as a byproduct of enzymatic processes.[1,2] HRP is known to be a monomeric glycoprotein (42 500 daltons) containing a single heme, iron(III) protoporphyrin IX. The carbohydrate is covalently bound and constitutes 18% of the mass of the protein.[1] The amino acid composition[3] and sequence[4] of HRP have been determined, and thus the primary structure of HRP is known, but little information is available on the secondary or tertiary structure of the protein. Glycoproteins such as HRP are difficult to crystallize, and the lack of satisfactory crystals has prevented a detailed X-ray structure of HRP from being obtained.[5] In the absence of X-ray data a variety of physicochemical methods, including ESR,[6] MCD,[7] resonance Raman,[8] as well as NMR spectroscopy,[9-12] have been used to characterize the heme pocket of HRP.

Previous NMR studies have yielded a wealth of information on the electronic/physical structure of the heme environment for both the ferric (largely high-spin) resting state of HRP[9] and the enzymatic intermediate ferryl compound I of HRP.[10] Less thoroughly studied have been the low-spin forms of ferric HRP. Three separate forms of low-spin ferric HRP have been identified.[11] In common with other heme proteins, HRP will coordinate added cyanide to form a ferric low-spin species; this form is designated HRPCN. Above pH 10.9, HRP, largely ferric high-spin, will convert to a ferric low-spin form; this form is

(1) Dunford, H. B.; Stillman, J. S. *Coord. Chem. Rev.* **1976**, *19*, 187-251.
(2) Caughey, W. S. In "Inorganic Biochemistry"; Eichorn, G. L., Ed.; Elsevier Scientific Publishing Company: Amsterdam, 1973; Vol. 2, Chapter 24.
(3) Welinder, K. G.; Smillie, L. B.; Schonbaum, G. R. *Can. J. Biochem.* **1972**, *50*, 44-62.
(4) Welinder, K. G. *Eur. J. Biochem.* **1979**, *96*, 483-502.
(5) Braithwaite, A. *J. Mol. Biol.* **1976**, *106*, 229-230.
(6) Colvin, J. T.; Rutter, R.; Stapleton, H. J.; Hager, L. P. *Biophys. J.* **1983**, *41*, 105-108.
(7) Nozawa, T.; Kobayashi, N.; Hatano, M.; Ueda, M.; Sogami, M. *Biochem. Biophys. Acta* **1980**, *626*, 282-290.
(8) Callahan, P. M.; Babcock, G. T. *Biochemistry* **1981**, *20*, 952-958.
(9) La Mar, G. N.; de Ropp, J. S.; Smith, K. M.; Langry, K. C. *J. Biol. Chem.* **1980**, *255*, 6646-6652.
(10) La Mar, G. N.; de Ropp, J. S.; Smith, K. M.; Langry, K. C. *J. Biol. Chem.* **1981**, *256*, 237-243.
(11) Morishima, I.; Ogawa, S.; Inubushi, T.; Yonezawa, T.; Iizuka, T. *Biochemistry* **1977**, *16*, 5109-5115.
(12) Williams, R. J. P.; Wright, P. E.; Mazza, G.; Ricard, J. R. *Biochem. Biophys. Acta* **1975**, *581*, 127-147.

0002-7863/84/1506-4438$01.50/0

Table I. Deuterated Protohemins

position (percentage) of deuteration	ref
1-C^2H_3 (60), 3-C^2H_3 (80)	20
1-C^2H_3 (60), 5-C^2H_3 (80)	20
2,4-α-C^2H (>90)	21
2,4-β-C^2H_2 (80–90)	21
$\alpha,\beta,\gamma,\delta$-*meso*-$^2H_4$ (60–70); 2,4-β-C^2H_2 (>90)	22
6,7-β-C^2H_2 (90)	23

abbreviated HRPa for HRP alkaline. Above pH 10.6 HRPCN, as we will show here, undergoes a transition to a form we designate HRPCN alkaline, abbreviated HRPCNa. Previous studies at lower field strengths reported spectra of ferric low-spin HRP complexes but could not assign resonances.[11,12] We report here high-field proton NMR studies of the three ferric low-spin complexes of HRP. Unambiguous assignment of heme resonances on the basis of specific isotope labeling permits quantitative comparison of the molecular/electronic structure in the heme cavity among the three forms and similar derivatives of the related cytochrome *c* peroxidase.

The ferric low-spin forms of HRP are not physiologically important, existing only above pH 10.5 or with cyanide present. However, these systems offer the advantage of well-resolved hyperfine shifted lines of comparatively small line width due to the fact that the iron spin $S = {}^1/_2$. Also, in contrast to the ferric state of HRP and the ferryl low-spin state of HRP-I, where the iron magnetic moment is essentially isotropic, ferric low-spin is highly anisotropic.[13] This leads to the possibility of resolving resonances of noncoordinated amino acids due to dipolar interaction with the iron. Hence, since the overall physical structure of the protein and specifically the heme pocket area should remain largely unaltered with changes in the iron state, the ferric low-spin states of HRP, especially HRPCN, offer an excellent probe of the heme pocket structure. Also, the low-spin ferric state of several other heme proteins has been well characterized by NMR,[14-16] facilitating comparison between their physical/electronic structures and those of ferric low-spin HRP. Finally, although a crystal structure of HRP is not available, that of the closely related protein cytochrome *c* peroxidase (CcP) is available.[17] Comparison of the spectra of HRPCN with the published and assigned spectra of CcPCN,[16] along with knowledge of the CcP crystal structure, permits tentative assignment of amino acid resonances in the heme pocket of HRP.

Experimental Procedures

Horseradish peroxidase, type VI, was purchased from Sigma as a lyophilized salt-free powder; the protein is predominantly isozyme C. The detailed purification, activity assay, and electrophoretic behavior of the protein used in this study have already been published,[9] as has the preparation of apo horseradish peroxidase and the reconstitution with a series of isotopically labeled protohemins.[9] The positions of deuteration of the heme are indicated by the square-bracketed prefix to the protein with use of the standard numbering scheme depicted in Figure 1. Table I lists the various deuterated hemins used in this study, the percent deuteration of the various sites, and the reference to the published synthetic procedure. All hemins used in this work were characterized by proton NMR of the ferric low-spin bis-cyanide form to determine identity, purity, and percent deuteration.

Solutions for proton NMR studies were 1 to 3 mM in protein in 0.2 M NaCl, 99.8% ^2H_2O. The solution pH, adjusted by using 0.2 M ^2HCl or 0.2 M NaO^2H, was measured with a Beckman 3550 pH meter equipped with an Ingold microcombination electrode. The pH was not corrected for the isotope effect and is hence referred to as "pH". HRPCN was formed by addition of excess KCN to a solution of HRP.

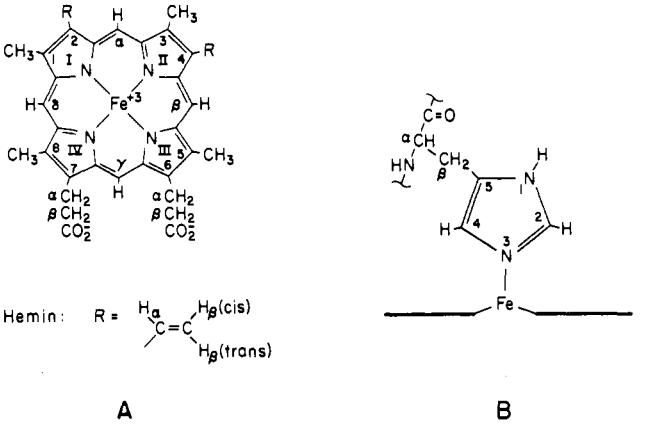

Figure 1. Structure and numbering system for (A) hemin and (B) the proximal histidine in HRP.

The 360-MHz proton NMR spectra were recorded on a Nicolet NT-360 Fourier transform NMR spectrometer operating with quadrature detection. Typical spectra consisted of 5000 pulses using 8192 data points over a 30 000-Hz bandwidth (9 μs 90° pulse). The residual water peak was suppressed by a 25-ms presaturation pulse; signal to noise was improved by exponential apodization which introduced 5–10 Hz line broadening. Peak shifts were referenced to the residual water line which in turn was calibrated against internal 2,2-dimethyl-2-silapentane-5-sulfonate (DSS). Chemical shifts are reported in parts per million, ppm, with downfield shifts taken as positive.

Line widths were determined for well-resolved peaks by use of the Nicolet computer subroutine LF which fits the peak to a Lorentzian line. For overlapping lines the routine NTCCAP was used. This routine enables the user to fit Lorentzian lines to the observed peaks. The line broadening introduced by apodization of the free induction decay was subtracted from all line width measurements.

Results

HRPCN. Figure 2A shows the low-field portion of the hyperfine shifted spectra of HRPCN, "pH" 7.0, in ^2H_2O at several temperatures. Downfield resonances are labeled a–j with a subscript to indicate the number of protons giving rise to a resonance, if determinable. Figure 2B presents expansion of the region 0 to −8 ppm at several temperatures. Upfield resonances are labeled a′–k′. At optimum resolution (55 °C) two downfield methyls a and b, and seven downfield single-proton resonances, c–i, are observed. The broad peak d lies directly under c at this pH; c and d are more clearly resolved at lower pH. Upfield of the diamagnetic region single-proton peaks a′–g′ and i′–k′ are observed, along with methyl h′. The intensity of h′ as a methyl was confirmed by use of computer simulation with NTCCAP. The temperature dependence of all resonances is shown in Figure 3 as Curie plots of shift vs. reciprocal temperature. All resonances treated show at least a slight decrease in shift at higher temperature consistent with their experiencing some hyperfine shift; diamagnetic intercepts at $T^{-1} = 0$ are given in parentheses to the left of each line.

A pH titration of HRPCN was conducted from "pH" 3 to 11.4. Figure 4 shows spectra at 35 °C over a range of "pH" values. It can be seen that above "pH" 10 HRPCN undergoes a transition slow on the NMR time scale to a new form characterized by overall smaller hyperfine shifts and designated HRPCNa. The "p*K*" was estimated as 10.6 from a comparison of the methyl peak areas of the two forms. In the low-pH range a fast-exchange transition is observed, with a "p*K*" of 4 as determined from a plot of shift vs. "pH" (not shown).[24] The origins of the two "p*Ks*"

(13) La Mar, G. N.; Walker, F. A. In "The Porphyrins"; Dolphin, D., Ed.; Academic Press: New York, 1979; Vol. 4, pp 61–157.
(14) La Mar, G. N.; Kong, S. B.; Smith, K. M.; Langry, K. C. *Biochem. Biophys. Res. Commun.* **1981**, *102*, 142–148.
(15) La Mar, G. N.; Burns, P. D.; Jackson, J. T.; Smith, K. M.; Langry, K. C.; Strittmatter, P. *J. Biol. Chem.* **1981**, *256*, 6075–6079.
(16) Satterlee, J. D.; Erman, J. E.; La Mar, G. N.; Smith, K. M.; Langry, K. C. *J. Am. Chem. Soc.* **1983**, *105*, 2099–2104.
(17) Poulos, T. L.; Freer, S. T.; Alden, R. A.; Edwards, S. L.; Skogland, U.; Takio, K.; Eriksson, B.; Xuong, N. T.; Yonetani, T.; Kraut, J. *J. Biol. Chem.* **1980**, *255*, 575–580.
(18) La Mar, G. N.; de Ropp, J. S.; Smith, K. M.; Langry, K. C. *J. Am. Chem. Soc.* **1983**, *105*, 4576–4580.
(19) de Ropp, J. S.; La Mar, G. N., manuscript in preparation.
(20) Smith, K. M.; Eivazi, F.; Langry, K. C.; Almeida, J. A. P. B.; Kenner, G. W. *Bioorg. Chem.* **1979**, *8*, 485–495.
(21) Budd, D. L.; La Mar, G. N.; Langry, K. C.; Smith, K. M.; Nayyir-Mazhir, R. *J. Am. Chem. Soc.* **1979**, *101*, 6091–6096.
(22) Smith, K. M.; Langry, K. C.; de Ropp, J. S. *J. Chem. Soc., Chem. Commun.* **1979**, 1001–1003.
(23) Langry, K. C. Ph.D. Thesis, University of California, Davis, 1981.

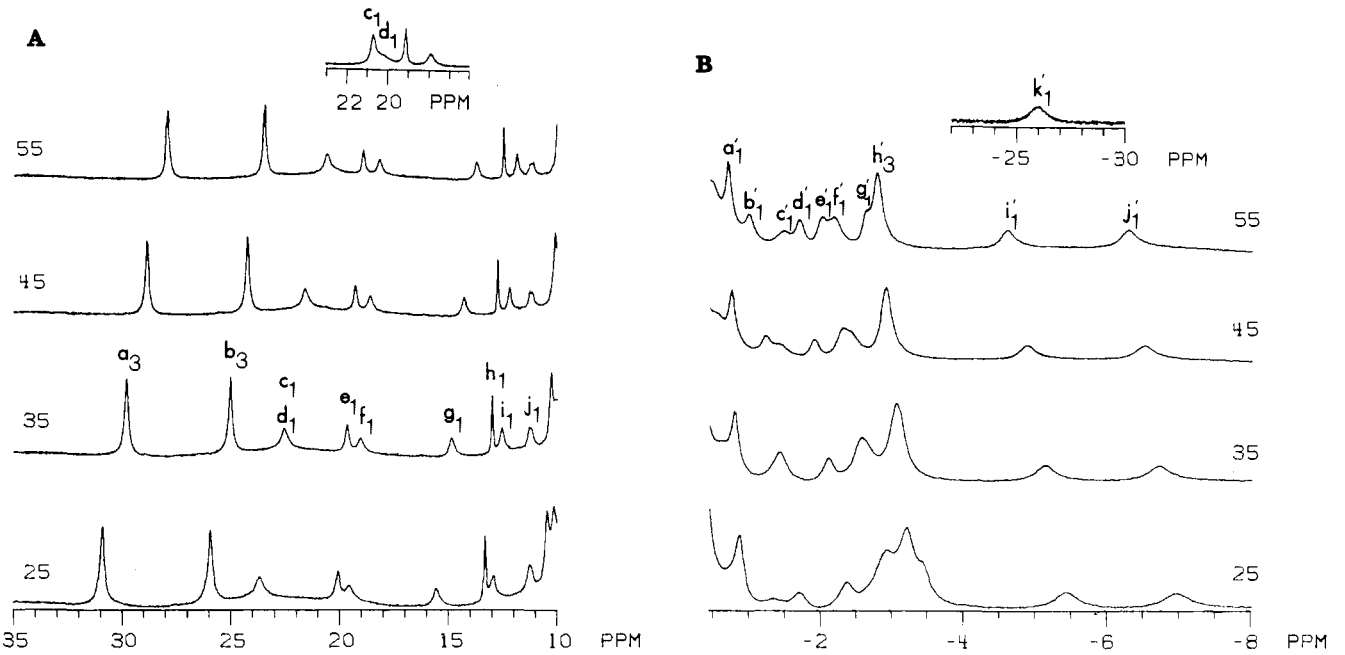

Figure 2. Hyperfine shifted portions of the 360-MHz spectra of HRPCN at "pH" 7.0 and the indicated temperatures: (A) downfield region and (B) upfield region. Peaks are labeled a–j downfield and a′–k′ upfield with a subscript to denote the number of protons contributing to a signal. The insert in A is at "pH" 5.1, 55 °C, and shows peaks c and d more clearly resolved. The insert in B shows the furthest upfield peak only at 55 °C.

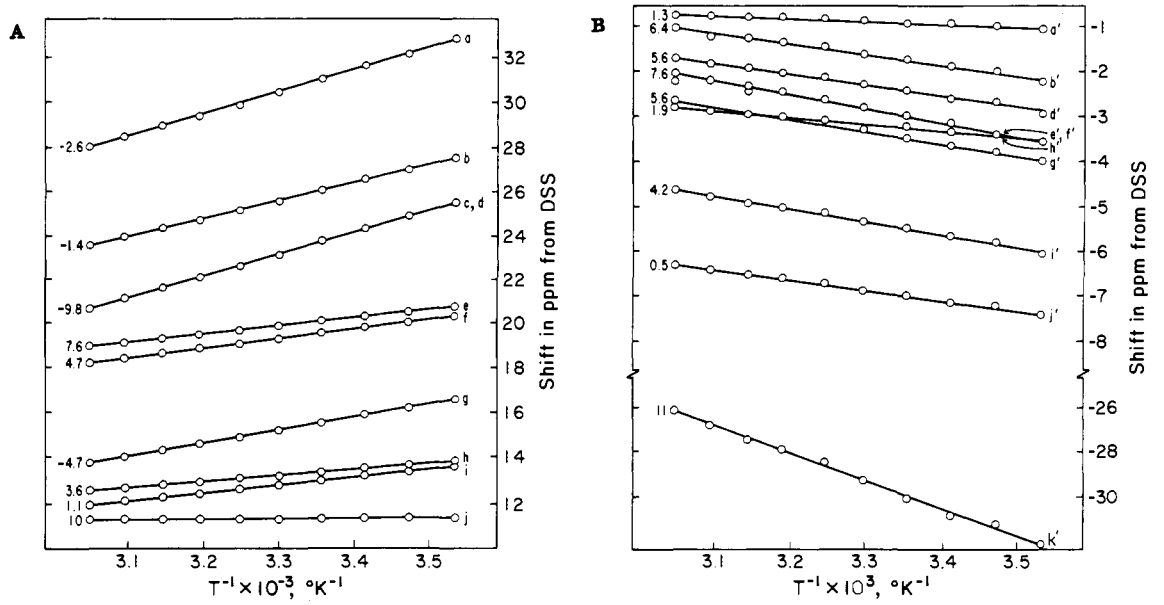

Figure 3. Curie plots of observed shift vs. reciprocal temperature for the resolved hyperfine shifted resonances of HRPCN in the (A) downfield and (B) upfield regions. The letter designation of each peak following the scheme of Figure 2 is given to the right of each line, and the extrapolated diamagnetic intercept at $T^{-1} = 0$ is given to the left.

will be discussed below.

Deuteration assignments were carried out by reconstituting various specifically deuterated hemins into apo-HRP and then obtaining spectra in the met-cyano form. Figure 5A shows the results of deuterium labeling for the downfield region of HRPCN at "pH" 7.0, 35 °C. Trace i shows unlabeled HRPCN while subsequent traces show labeled HRPCNs: (ii) [2,4-(α-C^2H)]-HRPCN and (iii) [4-α-C^2H]HRPCN. Trace i labels the peaks on the basis of the assignments made by traces ii and iii. The assignments of 8-CH_3 and 3-CH_3 are from an earlier work.[25]

Figure 5B shows the upfield HRPCN assignments at "pH" 7.0 (at 50 °C for greater resolution). Trace i is native HRPCN; subsequent traces show (ii) [2,4-(β-C^2H_2)]HRPCN, (iii) [2,4-(β-C^2H_2), $\alpha,\beta,\gamma,\delta$-*meso*-$^2H_4$]HRPCN, and (iv) [6,7-($\beta$-$C^2H_2$)]-HRPCN. The indicated assignments are labeled in trace i. Note that only one β-propionate and no meso peaks are detected. Table II lists chemical shifts and line widths for hyperfine shifted resonances of HRPCN.

HRPCNa. The titration of HRPCN with base results at high "pH" in a slow-exchange transition to a new form designated HRPCNa. The midpoint of the transition, based on methyl integrations, yields a "pK" of 10.6. The transition is illustrated in Figure 4. Deuteration assignments were carried out for HRPCNa at 35 °C as is illustrated in Figure 6A for the downfield region and Figure 6B for the upfield region. Figure 6A compares (i) native HRPCNa, (ii) [1,3-(C^2H_3)]HRPCNa, (iii) [1,5-(C^2H_3)]HRPCNa, and (iv) [2,4-(α-C^2H)]HRPCNa. Figure 6B compares (i) native HRPCNa, (ii) [2,4-(β-C^2H_2)]HRPCNa, (iii) [2,4-(β-C^2H_2),$\alpha,\beta,\delta,\gamma$-*meso*-$^2H_4$]HRPCNa, and (iv) [6,7-($\beta$-$C^2H_2$)]HRPCNa. The indicated assignments are labeled in each

(24) de Ropp, J. S. Ph.D. Thesis, University of California, Davis, 1981.
(25) La Mar, G. N.; de Ropp, J. S.; Smith, K. M.; Langry, K. C. *J. Am. Chem. Soc.* **1980**, *102*, 4833–4835.

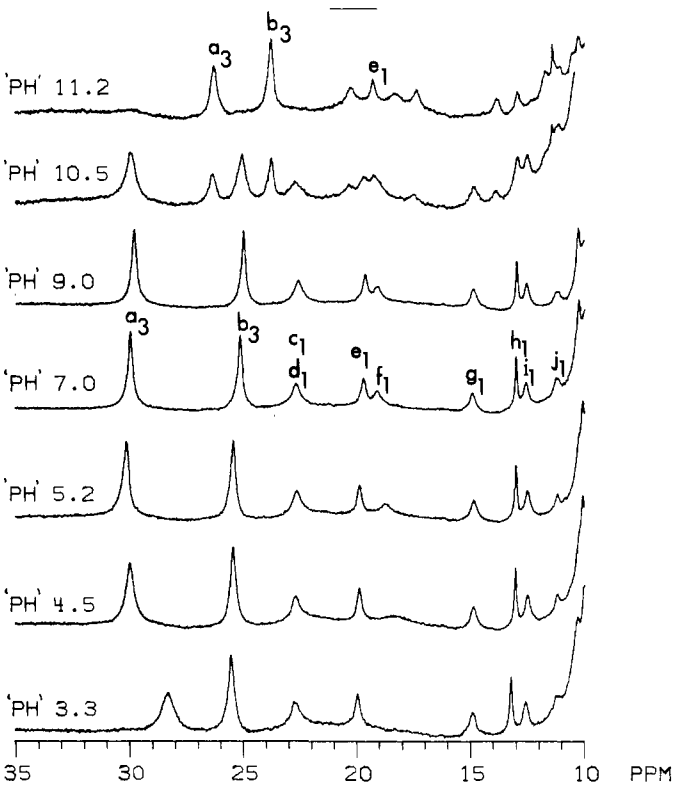

Figure 4. Downfield hyperfine shifted portions of the 360-MHz spectra of HRPCN at 35 °C as a function of "pH". Peaks in HRPCNa shown by deuterium labeling to be the same as peaks in HRPCN are so designated.

Table II. Observed Shifts, Line Widths, and Assignments for HRPCN at "pH" 7.0, 35 °C

peak designation[a]	assign[b]	shift,[c] ppm	line width,[d] Hz
a(3)	8-CH_3	29.76	64
b(3)	3-CH_3	24.97	60
c(1)	His-β-CH(?)	22.50	
d(1)	His 4'-H	22.50	>300
e(1)	4-α-CH	19.61	69
f(1)	7-α-CH	18.99	110
g(1)	His-β-CH(?)	14.82	120
h(1)		12.97	20
i(1)		12.50	56
j(1)		11.20	
a'(1)		−0.79	
b'(1)	2,4-β-CH	−1.43	
c'(1)		−1.43	
d'(1)	2,4-β-CH	−2.11	70
e'(1)	2,4-β-CH	−2.58	
f'(1)	6,7-β-CH	−2.58	
g'(1)	2,4-β-CH	−3.06	
h'(3)		−3.06	
i'(1)		−5.13	110
j'(1)		−6.71	110
k'(1)	His 2'-H	−28.37	320

[a] Peak designations are from Figures 2 and 3; the number of protons giving rise to the resonance is indicated in parentheses. [b] Assignments given in the table are unambiguous or reasonably certain; possible assignment of remaining peaks is treated in the Discussion. [c] Uncertainty in peak shifts ±0.02 ppm. [d] Estimated uncertainty in line widths ±10%. Line widths are given only for reasonably well resolved resonances.

figure. The methyls are assigned directly as 8–3. The α-vinyl, by comparison with HRPCN, must be 4-vinyl. Upfield three β-vinyls and a single β-propionate are detected, although it is not possible to say from which side chain they arise. Again no meso peaks are detected.

HRPa. The low-spin form of HRP, denoted HRPa, is obtained by raising resting state HRP above "pH" 10.9. Figure 7 illustrates the transition between HRP and HRPa. The process is slow on

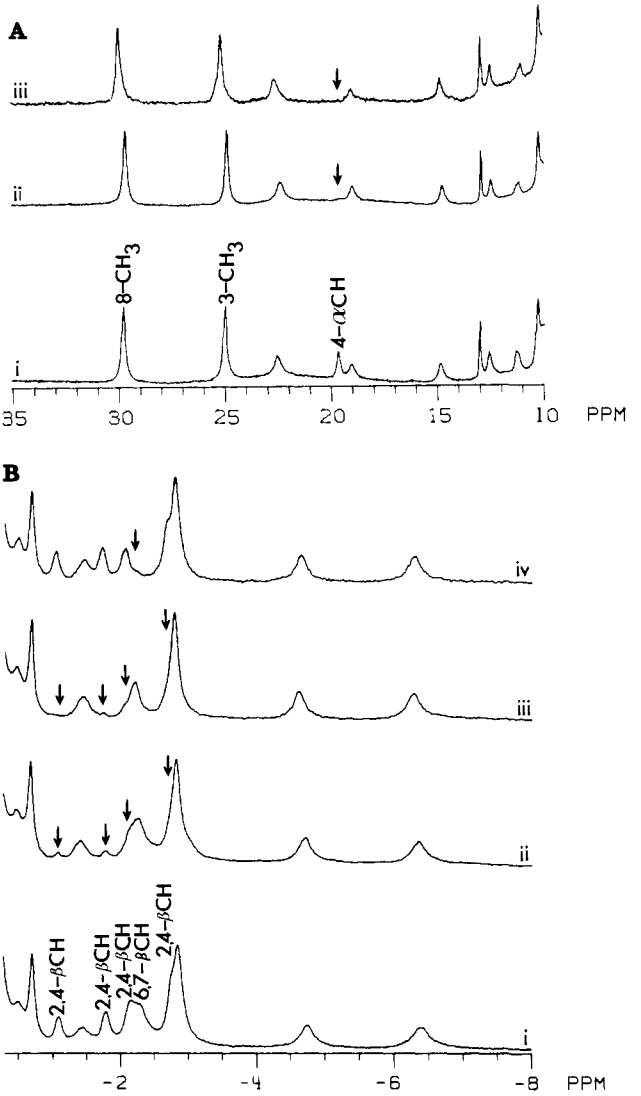

Figure 5. Assignments by specific isotope labeling of the 360-MHz spectrum of HRPCN at "pH" 7.0. Downfield assignments are shown at 35 °C in A: (i) native HRPCN, (ii) [2,4-(α-C^2H)]HRPCN, and (iii) [4-α-C^2H]HRPCN. Upfield assignments are shown at 50 °C in B: (i) native HRPCN, (ii) [2,4-(β-C^2H_2)]HRPCN, (iii) [2,4-(β-C^2H_2),α,β,-δ,γ-*meso*-$^2H_4$]HRPCN, and (iv) [6,7-(β-C^2H_2)]HRPCN. Peaks with clearly reduced intensities due to deuteration are marked with arrows, and assignments are given on the bottom (native HRPCN) trace.

the NMR time scale with a "pK" of 10.9. The spectral changes are even more pronounced in the absence of cyanide, since the enzyme converts from a largely high-spin form to a low-spin form with much smaller hyperfine shifts. Assignments were made at 35 °C, with Figure 8 illustrating the downfield assignments. Figure 8 compares (i) HRPa, (ii) [1,3-(C^2H_3)]HRPa, (iii) [1,5-(C^2H_3)]HRPa, and (iv) [2,4-(α-C^2H)]HRPa. The indicated assignments are given in trace i. Notable is the fact that the 1- and 5-CH_3 are now resolved downfield. The assignment of the α-vinyl as 2-α-vinyl follows from the fact that pyrrole I has a larger spin density than pyrrole II with 1-CH_3 experiencing significant hyperfine shift rather than 3-CH_3. The upfield portion of the spectrum is almost featureless, with only a shoulder to the diamagnetic envelope and no peaks detected at higher field than −4 ppm. No peaks disappeared upon deuteration in the upfield region (not shown).

Discussion

In the case of HRPCN the most appropriate model compounds are the well-characterized bis-cyano and mono-cyano, mono-imidazole Fe(III) low-spin hemins.[26,27] These models predict

(26) La Mar, G. N. In "Biological Applications of Magnetic Resonance"; Shulman, R. G., Ed., Academic Press: New York, 1979; pp 305–343.

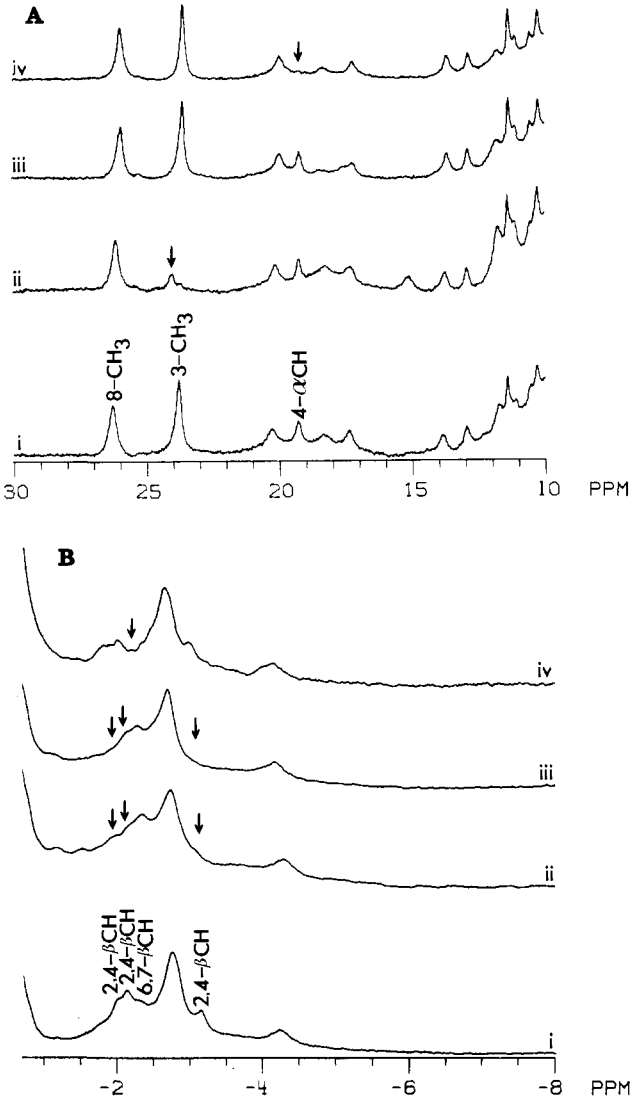

Figure 6. Assignments by specific isotope labeling of the 360-MHz spectrum of HRPCNa at "pH" 11.2 and 35 °C with A showing the downfield assignments [(i) native HRPCNa, (ii) [1,3-(C^2H_3)]HRPCNa, (iii) [1,5-(C^2H_3)]HRPCNa, (iv) [2,4-(α-C^2H)]HRPCNa] and B the upfield assignments [(i) native HRPCNa, (ii) [2,4-(β-C^2H_2)]HRPCNa, (iii) [2,4-(β-C^2H_2),α,β,γ,δ-*meso*-$^2H_4$]HRPCNa, (iv) [6,7-(β-C^2H_2)]-HRPCNa]. Peaks with clearly reduced intensities due to deuteration are marked with arrows, and assignments are given on the bottom (native HRPCNa) trace.

downfield shifts for the heme methyls, α-vinyls, and α-propionates, with β-vinyls, β-propionates, and meso protons all resonating upfield of the diamagnetic reference (i.e., in protoporphyrin IX zinc(II)). This pattern, observed previously in other ferric low-spin heme proteins,[14-16] is also present in HRPCN. As observed in other proteins, the heme resonances show greater shift asymmetry or spread. In particular, only two heme methyls, 8-CH_3 and 3-CH_3, and the 4-α-vinyl are observed and assigned by the deuterium labeling. The remaining α-vinyl at position 2 and the 5-CH_3 are presumably under the diamagnetic envelope 10 to 0 ppm. The primary mechanism for the large shift asymmetry in heme proteins relative to the models has been attributed to the interaction of the iron with the rigid proximal histidine, as opposed to the freely rotating ligands present in the model compounds, as will be elaborated below. This interaction places the maximum spin density on opposite pyrroles, either I and III, as in the case for sperm whale myoglobin cyanide (MbCN), or, as is the case for HRPCN, on pyrroles II and IV. Hence the substituents on

(27) Chacko, V. P.; La Mar, G. N. *J. Am. Chem. Soc.* **1982**, *104*, 7002-7007.

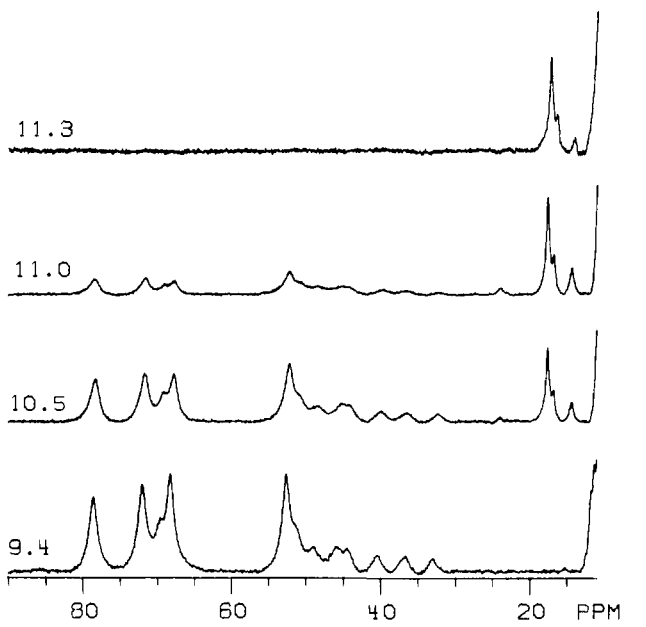

Figure 7. The transition from resting state HRP to HRPa illustrated by the downfield portions of the 360-MHz spectra of HRP at 35 °C and the indicated "pH" values. The characteristic resting state peaks at 30-80 ppm decrease and are replaced by new resonances above 20 ppm in the conversion to the alkaline form.

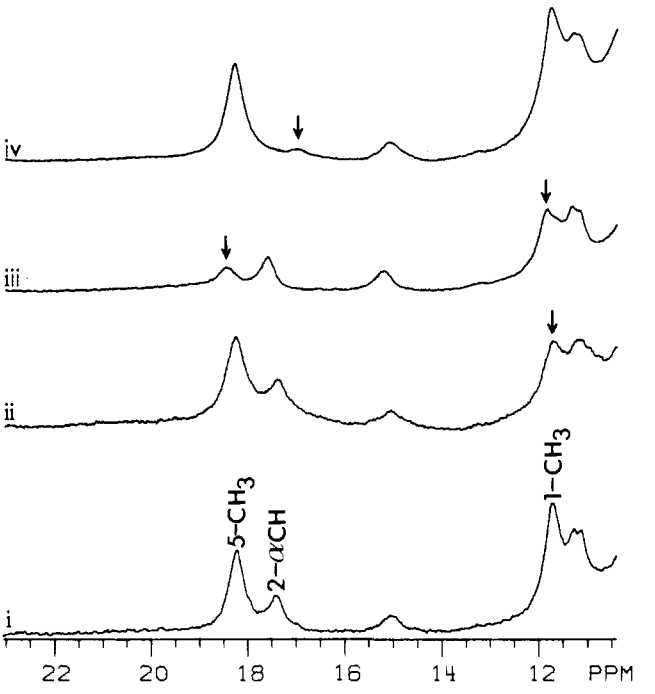

Figure 8. Assignments by specific isotope labeling of the downfield portion of the 360-MHz spectrum of HRPa at "pH" 11.2 and 35 °C: (i) native HRPa, (ii) [1,3-(C^2H_3)]HRPa, (iii) [1,5-(C^2H_3)]HRPa, and (iv) [2,4-(α-C^2H)]HRPa. Peaks with clearly reduced intensities due to deuteration are marked with arrows, and assignments are given on the bottom (native HRPa) trace.

these pyrroles show largest shift. The deuteration studies also assign all four β-vinyl resonances upfield (Figure 5B) as well as a β-propionate. This is presumably a 7-β-propionate based on the spin density arguments above. The assignment of the closely spaced β-vinyls to individual 2 and 4 side chains is not possible at this time. An attempt was made to assign the individual β-CH's by decoupling the 4-α-vinyl with a powerful selective pulse, but the β-vinyl resonances are so broad (ca. 70 Hz) that no line narrowing was detected. Only a single β-propionate resonance is detected and no meso peaks. The model ferric low-spin protohemins predict[26] these protons should resonate near or slightly

Table III. Shifts[a] of Peaks c and g in 2,4-R-HRPCN

2,4-R group	shift c	shift g
acetyl	23.06	16.89
vinyl	22.50	14.82
hydrogen	22.32	14.35
ethyl	21.54	14.08

[a] Data obtained at "pH" 7.0, 35 °C. Uncertainty in shifts ±0.01 ppm.

downfield of 0 ppm and hence are buried under the upfield diamagnetic shoulder.

Even after all possible assignments are made by deuteration, several peaks with significant hypefine shift remain. The deuterium labeling accounts for all heme positions except the α-propionates; but these can in certain cases[24] be assigned by pH behavior, since the propionate at neutral pH becomes protonated at acidic pH. The pH titration of HRPCN (Figure 4) reveals that at "pH" <5 the 8-CH_3 and peak f change shift and broaden. The observed "pK" of 4 corresponds well to the pK of the propionic acid side chain(s) as observed in other heme proteins.[5] This is corroborated by the fact that the 8-CH_3 at low pH shows much more significant shift and broadening than the 3-CH_3, which is distant from the 6,7 side chains. The reasonable assumption can be made that of the single-proton peaks those that experience the largest change in shift and line width at low pH will be the α- and β-propionates. The ferric low-spin models predict that α-propionates will resonate downfield with shifts ca. 7–8 ppm.[26] In the asymmetric protein environment the shifts of these resonances will be spread, just as for the methyls. Also, in the protein the methylene CH_2's will be diastereotopic, hence single-proton resonances will be observed for these groups. Thus by taking HRPCN to low pH, we observe one resonance, f, that exhibits marked shift and broadening due to rapid exchange between propionate and propionic acid forms. Since the 8-CH_3 shows larger hyperfine shift than the unresolved 5-CH_3, indicating larger spin density on pyrrole IV than pyrrole III, the α-propionate is assigned as a 7-α-propionate, thus placing the methyl and α-propionate of largest shift on the same pyrrole. The other 7-α-propionate is presumably in the diamagnetic envelope, as are the α-propionates of the 6 side chain.

In addition to the heme resonances, on the basis of model compound spectra we expect all the protons of the proximal histidyl imidazole including the β-CH_2 protons to experience significant hyperfine shifts, though the N_1H will not be observed due to exchange with ^2H_2O solvent. Inspection of the HRPCN data (Table II) reveals two resonances markedly broader than all others. Peaks d and k′ each have line widths in excess of 300 Hz and have already been assigned to the proximal histidyl imidazole 2-H and 4-H on the basis of dipolar relaxation and the change in their shift upon heme modification.[28]

Ferric low-spin models of the type PFe(CN)Im, where Im is a substituted 5-methylimidazole, predict that the β-CH_2 protons of the proximal imidazole should resonate downfield of 10 ppm.[27] In the protein environment these protons are diastereotopic and will give rise to two single-proton resonances. Hence two of the remaining unassigned downfield single-proton resonances could arise from the β-CH_2 group of the histidine, or one α-CH propionate resonance that does not titrate. Evidence that peaks c and g are perhaps β-CH_2 protons comes from observing the shift of these two protons as a function of heme 2,4-R group. The shift of the protons of the proximal imidazole is sensitive to the 2,4-R heme substituent.[13,27] Groups that are electron withdrawing relative to vinyls, such as acetyls, result in larger contact shifts due to stronger iron–imidazole interaction for imidazole protons in mono-cyano mono-imidazole diacetyldeuterohemin relative to models with identical axial ligands but vinyls at 2,4-R.[28] Also, 2,4-R groups electron donating relative to vinyls, protons (deuterohemin), or ethyl groups (mesohemin) cause reductions in the contact shift.[29] This trend is also observed for peaks c and g in HRPCN reconstituted with 2,4-R-substituted hemins (Table III). The shifts of c and g show a steady decrease as the electron-donating ability of 2,4-R decreases. The 7-α-propionate does not follow these trends, which adds additional weight to c and g being the β-CH_2 protons and not a non-titrating α-propionate. Finally, it has been noted that the shift of β-CH_2 protons is considerably more downfield in the ferric mono-cyano, mono-imidazolate models than for similar models with neutral imidazole, which places the 5-CH_3 at ca. 12 ppm.[27] The large downfield shift of the HRPCN β-CH_2 is consistent with the postulated partial imidazolate character of the proximal histidine in HRPCN.[28]

The upfield bias of the extrapolated intercepts (Figure 3A) at $T^{-1} = 0$ for peaks c and g relative to the other resonances is also consistent with their assignment as the β-CH_2 protons since the heme ring current will place these signals several ppm upfield of their normal resonance position. All other resonances have intercepts at or near the diamagnetic region, and the Curie plots are all linear. However, in model compounds and some heme proteins the Curie plots of α-vinyl and α-propionate resonances are curved due to changes in rotational orientation of the side chains with temperature.[30] The Curie plots of the α-vinyl and α-propionate (and all other resonances) in HRPCN follow strict Curie behavior over the temperature range observed, arguing for single relatively fixed side chain orientations without rotational mobility. These data indicate tight steric interactions between the heme and the apoprotein, as has been observed in other oxidation/spin states of HRP.[9,10] Further evidence for tight steric interactions has been found in proton NMR measurements of the interactions of 2,4-R-modified hemins with apo-HRP, arguing that the environment around all NMR observable side chains is tight, especially at the 2-vinyl position.[18] The tight steric interactions between vinyl side chains and the heme pocket have been described to lock the vinyl side chains coplanar with the heme. This configuration allows electron delocalization from the heme to the vinyls and is postulated to be of use in stabilizing the porphyrin cation radical in compound I of HRP.[18]

Even after all possible hyperfine shifted resonances are assigned by deuteration, pH effect, line width, or effect of 2,4-R substituent, several clearly resolvable hyperfine shifted resonances remain. Downfield these are h–j, while upfield there are h′–j′. All resonances due to the proximal histidine have been accounted for. In addition, all heme protons outside the diamagnetic envelope have likewise been assigned (vide supra). The remaining unassigned resonances most probably arise from protons on noncoordinated amino acids in the heme pocket experiencing dipolar hyperfine shift due to the paramagnetic iron anisotropy.[31] The assignment of these resonances is particularly challenging and also would be particularly informative given the lack of X-ray structural data for HRP. The only guide for assignments is the published X-ray crystal structure of CcP[17] and comparison of the known amino acid sequences of CcP[32] and HRP.[4] HRP, minus its carbohydrate content, is of similar molecular weight to CcP, which has no carbohydrate content. Both contain ferric protoporphyrin IX, catalyze the same reaction, and go through a similar two-step reaction, forming compounds I and II.

The overall homology of amino acid sequences between the two proteins is only 15%, but there are important homologies in the proximal and distal environments of the heme. In particular, both have a proximal histidine (His-170 in the HRP numbering scheme), a histidine at the distal site 42, an aromatic amino acid at 41, a leucine at 39, and an arginine at site 38. Eight other amino acids in the proximal sequence and one in the distal environment are also identical for the two enzymes. For CcP it has been postulated that the key residues for catalysis are the proximal and distal His, the arginine-38, and residue 41, which is a tryptophan

(28) La Mar, G. N.; de Ropp, J. S.; Chacko, V. P.; Satterlee, J. P.; Erman, J. E. *Biochem. Biophys. Acta* **1982**, *708*, 317–325.
(29) Chacko, V. P.; La Mar, G. N., unpublished observations.
(30) La Mar, G. N.; Viscio, D. B.; Gersonde, K.; Sick, H. *Biochemistry* **1978**, *17*, 361–367.
(31) Johnson, R. D.; Ramaprasad, S.; La Mar, G. N. *J. Am. Chem. Soc.* **1983**, *105*, 7205.
(32) Takio, T.; Titani, K.; Ericsson, L. H.; Yonetani, T. *Arch. Biochem. Biophys.* **1980**, *203*, 615–629.

in CcP. Poulos has recently proposed[33] a mechanism that emphasizes the involvement of these residues, particularly the distal ones, as the key to compound I formation for CcP. The X-ray structure of CcP shows that both the distal Trp and Arg side chains lie about 3.6 Å above the distal face of the heme. The side chain of the Arg extends over pyrroles III and IV. The indole ring of the Trp (which is replaced with a phenylalanine in HRP) is parallel to the heme plane above pyrrole II. Comparison of the spectra of the neutral pH forms of HRPCN and CcPCN[16] shows that CcPCN contains peaks similar in shift, intensity, and ratio of line widths to resonances h, h′, i′, and j′ in the spectrum of HRPCN. These resonances are most probably from protons of the invariant amino acids in the heme environment of the proteins, specifically Arg-38, Leu-39, and His-42. A route to exact assignment of these resonances in both proteins based on distance data obtained from analysis of dipolar T_1 relaxation times may be possible in the near future. The methyl h′ is tentatively assigned to the invariant Leu-39 and peaks i′ and j′ to the side chain CH_2 of the invariant Arg-38.

Alkaline Forms of Low-Spin HRP. The deuteration assignments show that in the transition from HRPCN to HRPCNa the resolved heme methyls and α-vinyl decrease in hyperfine shift while maintaining the same shift order. In addition, in the transition from deuterohemin-HRPCN to deuterohemin-HRPCNa, the 2,4-pyrrole protons show an average upfield shift of 0.7 ppm.[34] Further, the imidazole 2-H peak shows a downfield shift in the transition to the alkaline pH form. This pattern of chemical shift changes can be explained if one assumes the axial magnetic anisotropy of the iron is increased in the transition to the alkaline form. An increase in anisotropy will cause a larger dipolar shift resulting in heme protons shifting upfield while coordinated imidazole peaks move downfield.[13] A quantitative comparison of the chemical shift changes to axial geometric factors is not practical due to the fact that it is likely that rhombic as well as axial iron anisotropy[31] are altered in the transition. However, the qualitative trend is appropriate to an increase in axial anisotropy in HRPCNa.

The transition between neutral HRP and HRPa results in much larger changes in the spectra (Figure 7). The resolved heme methyl and α-vinyl shifts are even smaller in HRPa than in HRPCNa; no β-vinyl or β-propionate resonances shift out of the diamagnetic envelope, and there is no peak analogous to k′ resolved in the region above 0 ppm for HRPa.[35] In addition, the downfield methyl shift order in HRPa is 5–1, *opposite* to the HRPCN and HRPCNa order of 8–3. The large change in the spectrum observed for the transition of HRP to HRPa at "pH" ca. 10.9 must be due to a significant change in the heme electronic structure. In the HRP to HRPa conversion the spin state is changed from largely high-spin to low-spin, which means that the axial field strength around the iron is increased markedly. From the similarities of the NMR and ESR of HRPa to Mb(III) imidazole and hemichrome, a denatured form of Hb with a histidyl imidazole as iron, sixth ligand, it has been concluded[11] that in the conversion of HRP to HRPa a distal histidine, presumably His-42, coordinates as sixth ligand to the iron making it low-spin. For the case of cyanide-ligated HRP, the same titration occurs but the distal histidine does not displace the cyanide, as a comparison of the spectra of HRPa and HRPCNa shows. It is not known what residue(s) are titrated in this transition; the pK value is closest to the pK of the side chain of lysine.

It has been postulated that the pairwise orientation of methyls (8–3 or 5–1) observed in ferric low-spin heme proteins is due to the fixed orientation of the proximal histidyl imidazole relative to the heme.[36,37] The unpaired spin density on individual pyrroles will be orthogonal to the imidazole plane, resulting in pyrroles perpendicular to the imidazole plane having maximum unpaired spin density. Substituents on these opposite pyrroles will then have maximum shifts, resulting in a methyl shift order of 8–3 or 5–1 depending on the imidazole–heme orientation. This model has been demonstrated to account for assignments for those heme-proteins where both the heme methyl assignments and imidazole–heme orientation (by X-ray crystal study) are known.[37]

Thus in HRP an orientation of the imidazole plane above pyrroles I and III is predicted. The transition at "pH" 10.6 does not markedly alter the heme–imidazole orientation since the shift pattern of HRPCN and HRPCNa is the same. However, coordination of the second histidine in HRPa *reverses* the methyl shift order. This could in principle be due to the proximal histidyl imidazole rotating by 90°. However, this is extremely unlikely because of the large change in the orientation of the polypeptide chain near the proximal histidine that would be required. Rather, from the above theory one would predict that the second histidyl imidazole coordinates more nearly along pyrroles II and IV, opposite the proximal histidyl imidazole orientation. Further, the iron–distal imidazole interaction must be stronger than the iron–proximal imidazole interaction in order to reverse the shifts. A stronger interaction with the distal histidine could be expected if the imidazole was deprotonated simultaneous to coordination (pK for formation of a coordinated imidazolate is $\simeq 10.5$[38]). Thus we propose that the change in heme methyl assignments in HRPa arises from the coordination of the imidazolate ring of the distal histidine, with its π plane essentially perpendicular to that of the proximal histidyl imidazole.

Acknowledgment. This research was supported by grants from the National Institute of Health, HL-16087, HL-22252, and GM-26226.

Registry No. Peroxidase, 9003-99-0; heme, 14875-96-8.

(33) Poulos, T. L.; Kraut, J. *J. Biol. Chem.* **1980**, *255*, 8199–8205.
(34) de Ropp, J. S.; La Mar, G. N., unpublished observations.
(35) A broad, coordinated imidazole resonance above 0 ppm in HRPa may exist; however, the line widths of methyl and α-vinyl resonances in HRPa are ~2.5-fold greater than those in HRPCN. This would indicate that the histidyl imidazole 2-H and 4-H resonances would have line widths of the order of 1 kHz, which are probably too broad to detect.
(36) Shulman, R. G.; Glarum, S. H.; Karplus, M. *J. Mol. Biol.* **1971**, *57*, 93–115.
(37) Traylor, T. G.; Berzinis, A. P. *J. Am. Chem. Soc.* **1980**, *102*, 2844–2846.
(38) Gadsby, P. M. A.; Thomson, A. J. *FEBS Lett.* **1982**, *150*, 59–63.